Research article JHEP|Reports

Glycogen synthase kinase 3 activity enhances liver inflammation in MASH

Authors

Mireille Khoury, Qianqian Guo, Kunimaro Furuta, Cristina Correia, Chady Meroueh, Hyun Se Kim Lee, Khaled Warasnhe, Lucía Valenzuela-Pérez, Andrew P. Mazar, Iljung Kim, Yung-Kyun Noh, Heather Holmes, Michael F. Romero, Caroline R. Sussman, Kevin D. Pavelko, Shahidul Islam, Adebowale O. Bamidele, Petra Hirsova, Hu Li, Samar H. Ibrahim

Correspondence

ibrahim.samar@mayo.edu (S.H. Ibrahim).

Graphical abstract

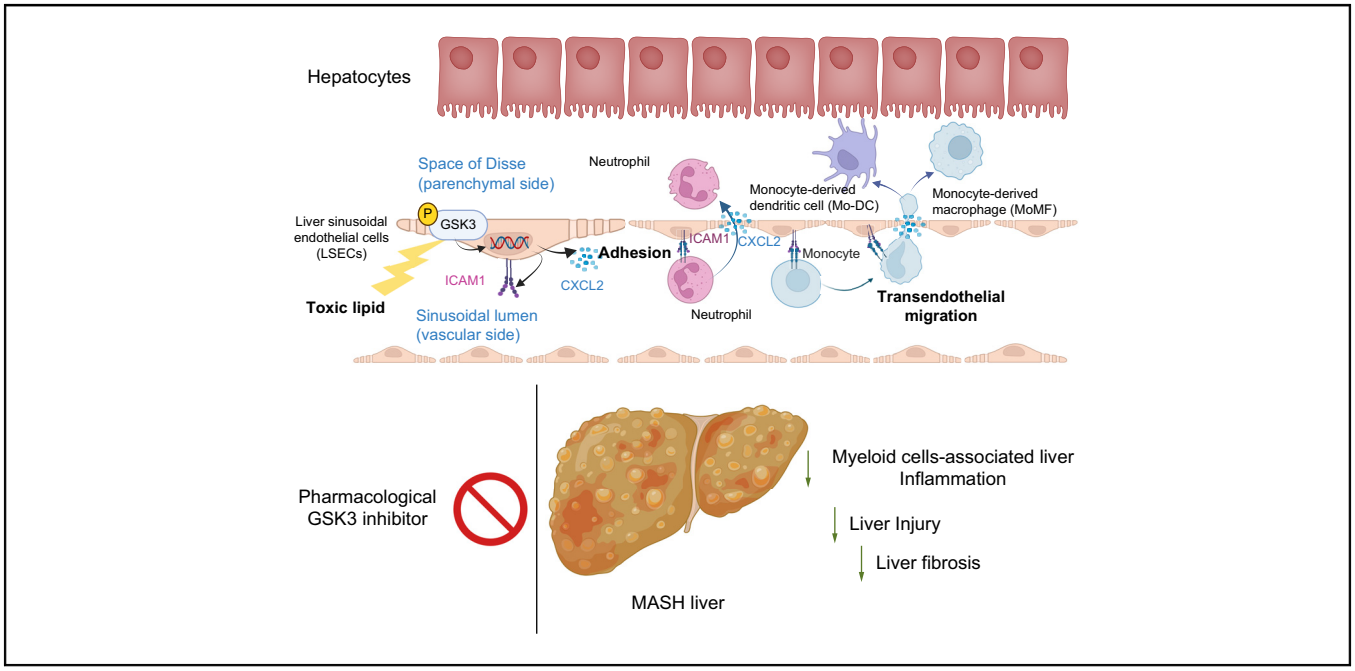

Highlights

- During MASH progression, LSECs under lipotoxic stress undergo proinflammatory changes, termed lipotoxic endotheliopathy.
- TEM and focal adhesion are among the top enriched pathways of differentially regulated genes (or protein-coding genes) in LSECs.
- GSK3β is the central hub kinase revealed by kinome profiling of the phosphoproteome of LSECs from mice with diet-induced MASH.
- GSK3 drives the toxic lipid-induced proinflammatory phenotype in LSECs.
- Pharmacological inhibition of GSK3 ameliorated liver inflammation, injury, and fibrosis in murine MASH.

Impact and Implications

LSECs under lipotoxic stress in MASH develop a proinflammatory phenotype known as endotheliopathy, with obscure mediators and functional outcomes. The current study identified GSK3 as the major driver of LSEC endotheliopathy, examined its pathogenic role in myeloid cell-associated liver inflammation, and defined the therapeutic efficacy of pharmacological GSK3 inhibitors in murine MASH. This study provides preclinical data for the future investigation of GSK3 pharmacological inhibitors in human MASH. The results of this study are important to hepatologists, vascular biologists, and investigators studying the mechanisms of inflammatory liver disease and MASH, as well as those interested in drug development.

https://doi.org/10.1016/j.jhepr.2024.101073

Research article

JHEP|Reports

Glycogen synthase kinase 3 activity enhances liver inflammation in MASH

Mireille Khoury,[1,†] **Qianqian Guo**,[1,†] Kunimaro Furuta,[1,2] Cristina Correia,[3] Chady Meroueh,[4] Hyun Se Kim Lee,[1] Khaled Warasnhe,[1] Lucía Valenzuela-Pérez,[1] Andrew P. Mazar,[5] Iljung Kim,[6] Yung-Kyun Noh,[6,7] Heather Holmes,[8] Michael F. Romero,[8,9] Caroline R. Sussman,[9] Kevin D. Pavelko,[10] Shahidul Islam,[1] Adebowale O. Bamidele,[1,11] Petra Hirsova,[1] Hu Li,[3] Samar H. Ibrahim[1,12,*]

[1]*Division of Gastroenterology & Hepatology, Mayo Clinic, Rochester, MN, USA;* [2]*Department of Gastroenterology and Hepatology, Osaka University Graduate School of Medicine, Osaka, Japan;* [3]*Center for Individualized Medicine, Department of Molecular Pharmacology and Experimental Therapeutics, Mayo Clinic College of Medicine and Science, Rochester, MN, USA;* [4]*Division of Anatomic Pathology, Mayo Clinic, Rochester, MN, USA;* [5]*Actuate Therapeutics Inc, Fort Worth, TX, USA;* [6]*Department of Computer Science, Hanyang University, Seoul, Republic of Korea;* [7]*School of Computational Sciences, Korea Institute for Advanced Study, Seoul, Republic of Korea;* [8]*Department of Physiology and Biomedical Engineering, Mayo Clinic, Rochester, MN, USA;* [9]*Division of Nephrology and Hypertension, Mayo Clinic, Rochester, MN, USA;* [10]*Immune Monitoring Core, Mayo Clinic, Rochester, MN, USA;* [11]*Department of Immunology, Mayo Clinic, Rochester, MN, USA;* [12]*Division of Pediatric Gastroenterology & Hepatology, Mayo Clinic, Rochester, MN, USA*

JHEP Reports **2024.** https://doi.org/10.1016/j.jhepr.2024.101073

Background & Aims: Metabolic dysfunction-associated steatohepatitis (MASH) is characterized by excessive circulating toxic lipids, hepatic steatosis, and liver inflammation. Monocyte adhesion to liver sinusoidal endothelial cells (LSECs) and transendothelial migration (TEM) are crucial in the inflammatory process. Under lipotoxic stress, LSECs develop a proinflammatory phenotype known as endotheliopathy. However, mediators of endotheliopathy remain unclear.

Methods: Primary mouse LSECs isolated from C57BL/6J mice fed chow or MASH-inducing diets rich in fat, fructose, and cholesterol (FFC) were subjected to multi-omics profiling. Mice with established MASH resulting from a choline-deficient high-fat diet (CDHFD) or FFC diet were also treated with two structurally distinct GSK3 inhibitors (LY2090314 and elraglusib [9-ING-41]).

Results: Integrated pathway analysis of the mouse LSEC proteome and transcriptome indicated that leukocyte TEM and focal adhesion were the major pathways altered in MASH. Kinome profiling of the LSEC phosphoproteome identified glycogen synthase kinase (GSK)-3β as the major kinase hub in MASH. GSK3β-activating phosphorylation was increased in primary human LSECs treated with the toxic lipid palmitate and in human MASH. Palmitate upregulated the expression of C-X-C motif chemokine ligand 2, intracellular adhesion molecule 1, and phosphorylated focal adhesion kinase, via a GSK3-dependent mechanism. Congruently, the adhesive and transendothelial migratory capacities of primary human neutrophils and THP-1 monocytes through the LSEC monolayer under lipotoxic stress were reduced by GSK3 inhibition. Treatment with the GSK3 inhibitors LY2090314 and elraglusib ameliorated liver inflammation, injury, and fibrosis in FFC- and CDHFD-fed mice, respectively. Immunophenotyping using cytometry by mass cytometry by time of flight of intrahepatic leukocytes from CDHFD-fed mice treated with elraglusib showed reduced infiltration of proinflammatory monocyte-derived macrophages and monocyte-derived dendritic cells.

Conclusion: GSK3 inhibition attenuates lipotoxicity-induced LSEC endotheliopathy and could serve as a potential therapeutic strategy for treating human MASH.

Impact and Implications: LSECs under lipotoxic stress in MASH develop a proinflammatory phenotype known as endotheliopathy, with obscure mediators and functional outcomes. The current study identified GSK3 as the major driver of LSEC endotheliopathy, examined its pathogenic role in myeloid cell-associated liver inflammation, and defined the therapeutic efficacy of pharmacological GSK3 inhibitors in murine MASH. This study provides preclinical data for the future investigation of GSK3 pharmacological inhibitors in human MASH. The results of this study are important to hepatologists, vascular biologists, and investigators studying the mechanisms of inflammatory liver disease and MASH, as well as those interested in drug development.

Keywords: Glycogen synthase kinase 3 (GSK3); Non-alcoholic steatohepatitis (NASH); Metabolic dysfunction associated steatohepatitis (MASH); Liver sinusoidal endothelial cells (LSEC); Myeloid cells; Inflammation; Chemokines; Adhesion; Migration; Liver fibrosis.

Received 6 June 2023; received in revised form 12 March 2024; accepted 20 March 2024; available online 26 March 2024

† These authors contributed equally to this work.

* Corresponding author. Address: Division of Pediatric Gastroenterology, Department of Pediatric and Adolescent Medicine, Mayo Clinic, 200 First Street SW, Rochester, MN 55905, USA. Tel.: +1 507 266 0114; Fax: +1 507 284 0160.

E-mail address: ibrahim.samar@mayo.edu (S.H. Ibrahim).

Introduction

Metabolic dysfunction-associated steatohepatitis (MASH) is a growing public health problem,[1] and its pathogenesis involves both lipotoxicity (toxic lipid-induced cellular stress)[2] and a sterile inflammatory response.[3] Similar to other liver cell types affected in MASH, lipotoxicity in liver sinusoidal endothelial cells (LSECs) triggers aberrant signaling, resulting in structural and functional alterations leading to LSEC dysfunction and a proinflammatory phenotype, which we refer to here as endotheliopathy.[4–6] Emerging data implicate LSEC endotheliopathy in liver inflammation in MASH.[7,8] Increased LSEC capillarization has been reported in mice with diet-induced MASH, as evidenced by reduced fenestrae and Lyve 1 expression (a marker of well-differentiated LSECs), and increased CD34 expression (a marker of capillarized LSECs).[9] In the current study, we examine the molecular mediators and functional outcome of lipotoxic LSEC endotheliopathy as it relates to MASH pathogenesis.

The inflammatory response in MASH is mainly mediated by recruited proinflammatory myeloid cells and their homing to the MASH liver.[10,11] Two of the crucial mechanisms involved in this process are the chemotaxis and adhesion of myeloid cells to LSECs.[12] Although a growing body of evidence implicates LSEC dysfunction in various liver diseases, including MASH,[13] few studies have focused on targeting molecular mediators of myeloid cell adhesion to LSECs in MASH.[7,14] Circulating myeloid cells exit the vasculature to achieve residence in the MASH liver, a process known as transendothelial migration (TEM). TEM is often preceded by leukocyte adhesion, a crucial step in the inflammatory response. It occurs via the paracellular route (at the adherence junction) or transcellular route (through transcellular channels). Paracellular TEM, the most common route of TEM for myeloid cells, is mediated by the disassembly of the adherence junctions.[15] Most leukocytes that adhere to the endothelial wall at the site of inflammation re-enter the circulation. However, once leukocytes commit to TEM, they migrate through the hepatic parenchyma to fuel the inflammatory process.[16]

Glycogen synthase kinase (GSK)-3 is a primary serine/threonine kinase that integrates multiple signaling pathways, including cell metabolism, adhesion, and inflammation.[17] It has two ubiquitously expressed and highly conserved isoforms (α and β), with both shared and distinct substrates and functional effects. Aberrant GSK3 activation is pathogenic in numerous inflammatory diseases, and GSK3 inhibitors in rodent models have been successful in curtailing exuberant inflammatory responses.[18,19] Furthermore, GSK3β has been implicated in pulmonary vascular endothelial barrier dysfunction.[20] In addition, GSK3α promotes fatty acid uptake and lipotoxic cardiomyopathy in murine models of diet-induced obesity.[21] However, the biological consequences of lipotoxicity-induced aberrant GSK3 activation in LSEC, as well as the potential therapeutic ramifications of inhibiting GSK3 enzymatic activity during MASH, are largely unknown.

Herein, using phosphoproteomics and kinome profiling in mouse LSECs, we report that GSK3β serves as a major hub and the main kinase in MASH, thereby acting as a potential driver of lipotoxic endotheliopathy. Furthermore, we show that GSK3β in LSECs mediates key elements of TEM: (i) expression of chemokines, namely C-X-C motif chemokine ligand (CXCL)-2; and (ii) density of adhesion molecules, namely intracellular adhesion molecule 1 (ICAM-1). Most importantly, using established diet-induced mouse models of MASH, we identified that pharmacological inhibition of GSK3 using two structurally distinct inhibitors that have been used in human clinical trials (NCT01287520 and NCT04218071) ameliorates liver injury, inflammation, and fibrosis, mainly by reducing myeloid cell infiltration into the liver.

Materials and methods

The full details of the materials and methods are provided in the supplementary data online.

Results

GSK3β is the top hub kinase altered in MASH LSECs

To obtain a comprehensive and in-depth understanding of the LSEC phenotype and intracellular signaling networks during MASH, we performed phospho- and total proteomic analyses on LSECs isolated from mice fed either a chow or a fat, fructose, and cholesterol (FFC) diet for 24 weeks. The FFC diet is a well-established MASH mouse model that phenocopies the metabolic and histological features of the human disease (Fig. 1A).[7,22] We performed an integrated pathway analysis of the total proteomic data and our previously generated LSEC transcriptomic data (GSE164006).[7] We selected genes (or protein-coding genes) that were differentially regulated between chow-fed and FFC-fed mice using LSEC total proteomic or RNA-sequencing (RNA-seq). We reasoned that focusing on genes showing consistent directionality changes in both layers of 'omics' might provide insights into the underlying biological aspects of the disease. Hence, we subjected all mRNA-protein correlated genes (orange and blue dots in Fig. 1B) to a Kyoto Encyclopedia of Genes and Genomes (KEGG) over-representation pathway analysis (Fig. 1C). We identified leukocyte TEM (p = 5.96E-04) and focal adhesion (p = 2.94E-04) among the top-10 canonical pathways altered in MASH LSECs. These findings are consistent with emerging literature implicating monocyte adhesion to endothelial cells and TEM in the sterile inflammatory process in MASH.[23] Next, we performed kinome enrichment analysis[24] of the LSEC phosphoproteomic data based on the phosphorylation status of putative substrates of kinases. Notably, GSK3β was identified as the major hub (Fig. 1D) on the kinome map and the top-ranked kinase with altered activity in MASH (p = 1.58E-03) (Fig. 1E and Fig. S1). To further confirm the findings obtained from murine phosphoproteomics and explore their relevance to human biology, we examined whether GSK3 is activated in human LSECs under lipotoxic stress. To this end, we used the saturated free fatty acid (FFA) palmitate (PA) to induce lipotoxicity *in vitro*. PA contributes to the majority of circulating saturated FFA in human MASH,[25] and its lipotoxic impact on LSECs has been previously established.[7] First, we showed in primary human LSECs that phosphorylation of tyrosine residues (Y279 for GSK3α and Y216 for GSK3β), which are known to enhance the enzymatic activity of both GSK3[26] and glycogen synthase (GS), a specific GSK3 substrate, increased with PA treatment. Furthermore, GS phosphorylation in primary human LSECs was reduced by treatment with the GSK3 pharmacological inhibitor LY2090314 (LY) (Fig. 1F). Likewise, in a mouse LSEC cell line, known as transformed mouse LSECs (TSECs), phosphorylation of GSK3α/β (Y279/216) and GS was increased by PA treatment (Fig. 1G). We

also confirmed the sequential phosphorylation of GSK3 and GS using TSECs treated with the FFA toxic intracellular metabolite lysophosphatidylcholine (LPC) (Fig. 1H).[27] Collectively, these findings confirm that GSK3 is activated in human and mouse LSECs under lipotoxic stress and in mice with diet-induced MASH.

GSK3 mediates toxic lipid-induced proinflammatory responses in LSECs

Next, we investigated whether toxic lipid-induced GSK3 activation promotes LSEC proinflammatory phenotypes. To obtain a comprehensive human LSEC transcript data set, we treated primary human LSECs with (i) vehicle (Veh), (ii) PA, or (iii) PA with LY, and subjected the isolated RNA to a NanoString-based mRNA profiling assay, which can quantify the copy numbers of 760 fibrosis-related human genes.[28] In total, 479 genes were detected, 31 of which were abundant in cells treated with PA *vs.* Veh and categorized as 'lipotoxic stress-dependent genes', and 154 genes were upregulated in cells treated with PA *vs.* PA with LY and categorized as 'GSK3-dependent genes' (Fig. 2A). To further narrow down the gene candidates that are likely essential in MASH pathogenesis across human and mouse species, we used our LSEC RNA-seq data from FFC diet-induced MASH. Genes upregulated in MASH *vs.* chow mice were categorized as 'MASH-

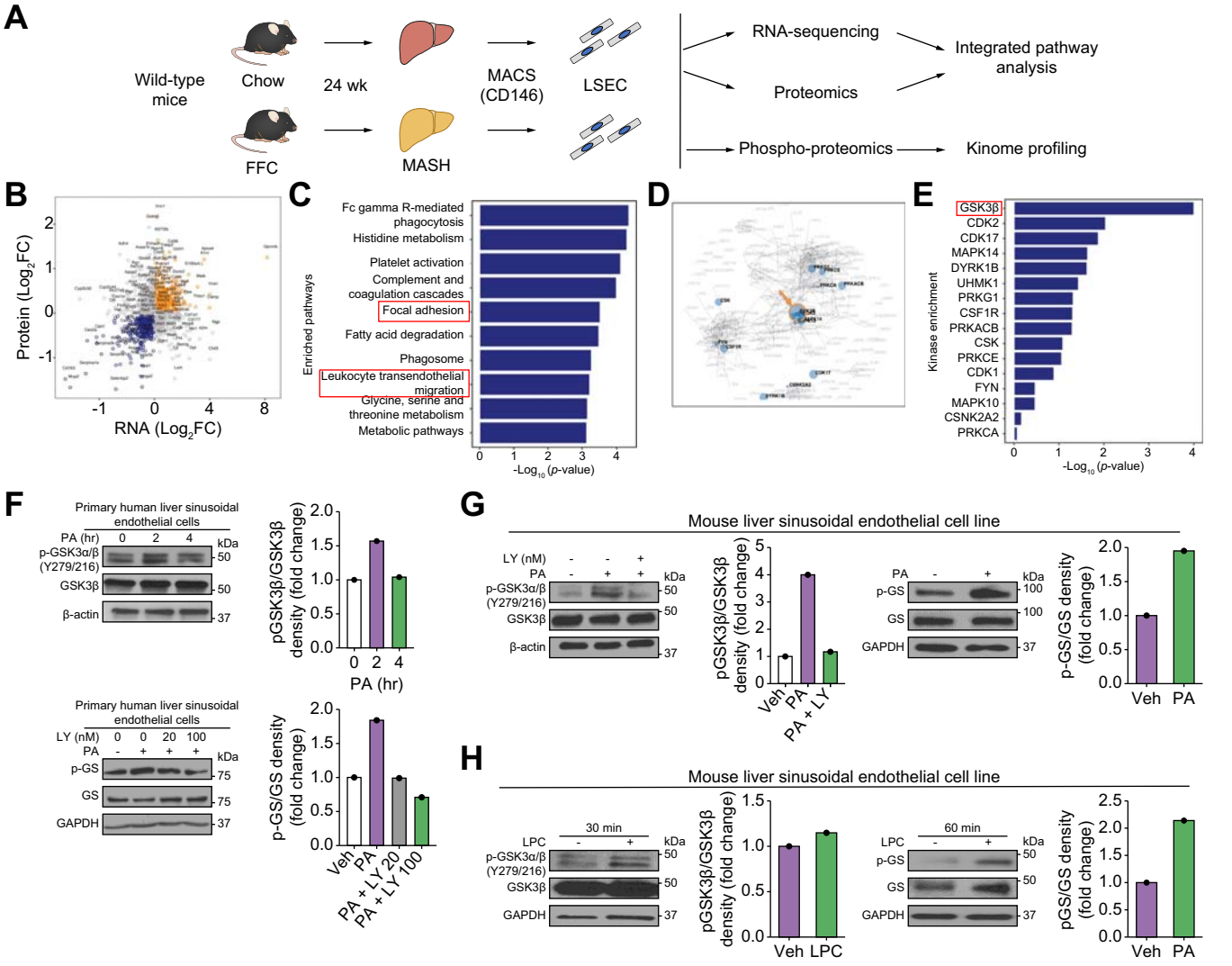

Fig. 1. Glycogen synthase kinase (GSK)-3β is a central mediator of liver sinusoidal endothelial cell (LSEC) endotheliopathy in metabolic dysfunction-associated steatohepatitis (MASH). (A) Schematic of the *in vivo* multi-omics study. (B) Scatter plot showing differentially expressed genes (p <0.05) in chow *vs.* fat, fructose, and cholesterol (FFC)-fed mice based on either LSEC total proteomic or RNA-sequencing (RNA-seq) analysis. The x- and y-axes represent the log 2-converted fold change (log_2FC) of the signals in FFC- *vs.* chow-fed mice in the proteomic and RNA-seq studies, respectively. (C) Top-10 enriched pathways representative of the differentially regulated genes in FFC *vs.* chow-fed mice based on both proteomics and RNA-seq analyses. (D) Kinome map generated from the phosphoproteomic study shown in A. (E) Top-16 ranked putative altered kinases in FFC *vs.* chow-fed mice. (F) Primary human LSECs were treated with the vehicle (Veh), 500 μM palmitate (PA), or 500 μM PA ± the GSK3 inhibitor LY2090314 (LY). Protein levels of phosphorylated (p)-GSK3α/β (Y279/216) and GSK3β (top) and phosphorylated glycogen synthase (p-GS) and glycogen synthase (GS) (bottom) were assessed using Western blotting. (G) A mouse LSEC line was treated with Veh or 500 μM PA ± 20 nM LY for 4 h, and the protein levels of p-GSK3α/β (Y279/216) and GSK3β were assessed (left). Mouse LSEC lines were also treated with Veh or 500 μM PA for 2 h and p-GS and GS were assessed. (H) A mouse LSCE line was treated with Veh or lysophosphatidylcholine (LPC), and the protein levels of p-GSK3α/β (Y279/216), GSK3β, p-GS, and GS were assessed. β-Actin or glyceraldehyde-3-phosphate dehydrogenase (GAPDH) was used as loading control. F–H were repeated for at least three times; representative results are shown with quantification.

dependent genes'. Ten genes overlapped among the three categories defined above. Among these, we focused on *ICAM1* and *CXCL2*, which encode the adhesion molecule ICAM-1 and CXCL2, respectively. Our selection was based on the potential of ICAM-1 and CXCL2 acting in concert during myeloid cell transmigration across the sinusoidal endothelium. These findings were confirmed by conventional quantitative (q)PCR, showing the upregulation of *ICAM1* and *CXCL2* in PA-treated LSECs and the reduction in expression of these genes by inhibition of GSK3 function with LY treatment or GSK3β small interfering (si)RNA transfection (Fig. 2B and D). Interestingly, the increased expression of *ICAM1* and *CXCL2* induced by the proinflammatory cytokine tumor necrosis factor (TNF)-α was not reduced by GSK3 inhibition (Fig. 2C), suggesting that GSK3 selectively promotes the proinflammatory phenotype in LSECs downstream of the lipotoxic signal.

To assess the zonal distribution of lipotoxic endotheliopathy across the hepatic lobule *in vivo*, we used ICAM-1 as a marker of MASH endotheliopathy and scanned whole *ICAM1*-immunostained slides from mice with FFC diet-induced MASH and chow controls. The liver pathologist manually annotated the zones of the liver lobules and used a machine learning algorithm to analyze the zonal changes in *ICAM1* expression (Fig. S2A and B), showing no zonal difference in the expression of *ICAM1* or the percentage of steatotic area (Fig. S2C). These findings suggest that LSEC endotheliopathy in MASH is present across all liver zones. To confirm that the role of GSK3 in MASH pathogenesis is conserved in human disease, we performed Western blotting on

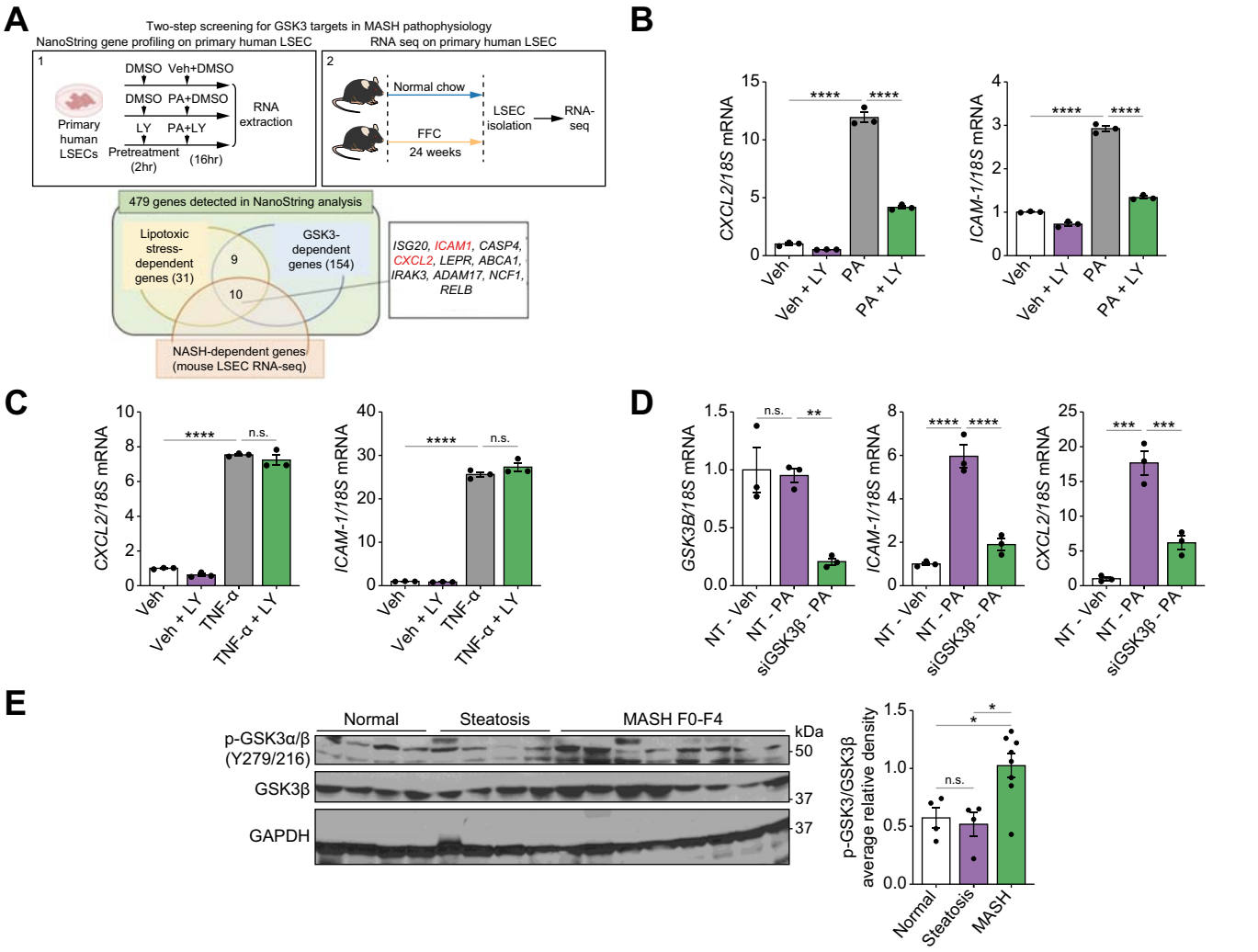

Fig. 2. Glycogen synthase kinase (GSK)-3 mediates toxic lipid-induced proinflammatory responses in liver sinusoidal endothelial cells (LSECs). (A) Primary human LSECs were treated with vehicle (Veh) or 500 μM palmitate (PA) ± 20 nM LY2090314 (LY) for 16 h, and gene expression profiling was performed using the NanoString nCounter system (1). LSECs were isolated from chow- and fat, fructose, and cholesterol (FFC)-fed mice and subjected to RNA-sequencing (RNA-seq) (2). Venn diagram (bottom) of genes classified as 'lipotoxic stress-dependent genes' and 'GSK3-dependent genes' in NanoString analysis and 'Metabolic dysfunction-associated steatohepatitis (MASH)-dependent genes' in mouse LSEC RNA-seq. Primary human LSECs were treated with Veh or 500 μM of PA (B) or 10 ng/ml tumor necrosis factor (TNF)-α (C) ± 20 nM LY for 16 h, and mRNA expression of C-X-C motif chemokine ligand 2 (*CXCL2*) and intracellular adhesion molecule 1 (*ICAM1*) was examined. (D) Primary human LSECs were transfected with siGSK3β or non-target small interfering (si)RNA for 72 h, then treated with Veh or 500 μM PA for 24 h, and the mRNA expression of *GSK3B*, *CXCL2*, and *ICAM1* was examined (n = 3 per group). (E) Phospho-GSK3α/β (Y279/216) and GSK3β protein levels were assessed in normal controls and patients with steatosis, and MASH by Western blotting with quantification. Glyceraldehyde-3-phosphate dehydrogenase (GAPDH) was used as the loading control (n = 4–8 per group). Bar graphs represent mean ± SEM; $^{*}p$ <0.05, $^{**}p$ <0.01, $^{***}p$ <0.001, $^{****}p$ <0.0001, ns, non-significant (one-way ANOVA with Bonferroni's multiple comparison).

human liver samples and confirmed increased GSK3α/β (Y279/216) phosphorylation in patients with MASH compared with patients with steatosis and normal subjects (Fig. 2E). Collectively, these observations support the concept that GSK3 activation promotes a proinflammatory phenotype in LSECs under lipotoxic stress, culminating in endotheliopathy.

GSK3 activation in LSECs under lipotoxic stress enhances myeloid cell adhesion and TEM

TEM of myeloid cells is a key biological process in their recruitment to sites of inflammation, and is associated with reduced endothelial barrier integrity.[15] Activated focal adhesion kinase (FAK) in endothelial cells promotes the phosphorylation of vascular endothelial cadherin (VE-cadherin). Phosphorylated VE-cadherin dissociates from β-catenin, leading to the displacement of β-catenin from cell adherens junctions, widening of cell–cell junctions, and disruption of endothelial barrier integrity (Fig. 3A).[29] Given that FAK is a known substrate of GSK3, we sought to determine the effect of activated GSK3 on FAK phosphorylation in LSECs under lipotoxic stress. We found that PA treatment enhanced FAK phosphorylation in LSECs, which was attenuated by GSK3 inhibition with LY (Fig. 3B). Enhanced phosphorylation of FAK during lipotoxic stress in a GSK3-dependent manner was also associated with increased VE-cadherin phosphorylation (Fig. 3B) and intracellular expression (Fig. 3C). Moreover, we observed reduced β-catenin intensity around the cell–cell junction in response to PA (Fig. 3D), which is suggestive of adherens junction disassembly essential for TEM and hepatic infiltration of recruited myeloid cells during MASH.

Next, we examined whether toxic lipid-induced activation of GSK3 in LSECs enhanced myeloid cell adhesion and TEM. A flow-based adhesion assay (Fig. 3E) showed reduced adhesion of primary human neutrophils to LSECs pretreated with PA and LY. Next, we assessed the impact of GSK3 inhibition on the TEM of myeloid cells through an LSEC monolayer under lipotoxic stress. The TEM assay using a Transwell system with a porous membrane-assembled insert has intrinsic limitations in that the fluid media at the bottom chamber does not reproduce well the

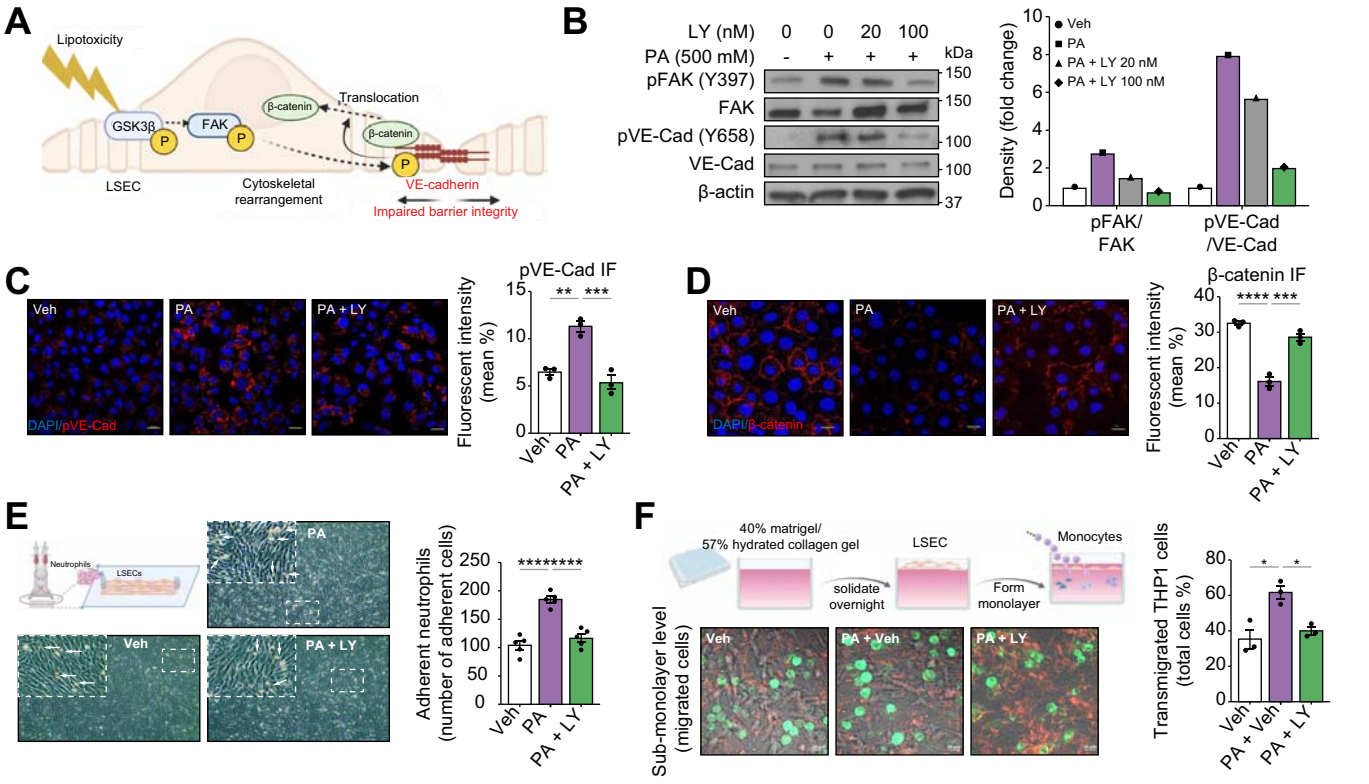

Fig. 3. Glycogen synthase kinase (GSK)-3 mediates liver sinusoidal endothelial cell (LSEC) lipotoxicity-induced monocyte transendothelial migration (TEM). (A) Schematic showing that lipotoxicity-induced GSK3β activation triggers a multistep phosphorelay signal transduction mechanism (GSK3β–focal adhesion kinase [FAK]–vascular endothelial [VE]-cadherin), leading to LSEC cytoskeletal rearrangement, adherence junction disassembly, and β-catenin dissociation from VE-cadherin and internalization, resulting in endothelial barrier dysfunction. (B) Primary human LSECs were treated with vehicle (Veh) or 500 μM palmitate (PA) ± LY2090314 (LY) at the indicated concentrations for 4 h, and protein levels of phosphorylated FAK (p-FAK), total FAK, phosphorylated (p)-VE-cadherin, and total VE-cadherin were assessed by Western blotting. β-Actin was used as a loading control. B was repeated at least three times, and representative results are shown, along with quantification. (C) Localization of p-VE-cadherin was assessed using immunofluorescence and quantified (right). (D) β-Catenin localization was assessed by immunofluorescence and quantified (right). DAPI was used for the nuclear staining. (E) Schematic of the flow-based neutrophil adhesion assay. Representative microscopic images of neutrophils adherent to primary human LSECs under the three experimental conditions. White arrows indicate adherent neutrophils. Five random fields in a 20 × microscopic field for each condition were captured and quantified (right). (F) Schematic of the collagen gel-based TEM assay. Representative images from confocal microscopy for the TEM assay at 1 h (left). THP-1 cells (green fluorescence) in focus on the apical surface of the endothelial monolayer (red fluorescence) were defined as non-migrated, those in focus below the plane of the endothelial monolayer were defined as transmigrated, and three random fields in a 63 × microscopic field from each condition were captured and quantified. Bar graphs represent mean ± SEM; $^{*}p$ <0.05, $^{**}p$ <0.01, $^{***}p$ <0.001, $^{****}p$ <0.0001 (one-way ANOVA with Bonferroni's multiple comparison; n = 3–5 per group). Scale bars: 20 μm (C,D,F).

colloidal extracellular matrix of the space of Disse, and LSECs plated on the membrane can migrate through the pore, which complicates the analysis of the data. Hence, we utilized a previously used system with minor modifications to mimic the liver sinusoidal milieu; Vybrant DiI-labeled LSECs were plated directly onto a hydrated collagen gel to form a monolayer, and the migration of the DiO-labeled monocytic cell line THP-1 was assessed using confocal microscopy.[30] Our data indicated an increase in the number of THP-1 cells that migrated through the Veh-pretreated LSEC monolayer into the collagen gel in response to PA treatment, in contrast to LSEC pretreated with LY20930314, where there was a significant reduction in migrated THP-1 cells, suggesting that myeloid cell TEM in response to lipid-induced signals in LSECs is mediated by intrinsic GSK3 enzymatic activity (Fig. 3F). Taken together, these data support a crucial role for LSEC GSK3 during lipotoxicity in myeloid cell TEM.

GSK3 inhibition with LY2090314 ameliorates FFC diet-induced murine MASH

Based on our *in vitro* findings supporting the proinflammatory role of aberrant GSK3 activation in LSECs under lipotoxic stress, we examined the potential beneficial effect of GSK3 inhibition in mice with FFC diet-induced MASH. Chow- or FFC-fed mice were treated with Veh or the GSK3 inhibitor LY three times a week for 4 weeks (Fig. 4A). We elected to use LY given its established safety and tolerability in humans.[31] First, we examined the metabolic phenotypes of these mice. Daily caloric intake, body weight, and homeostasis model assessment of insulin resistance (HOMA-IR) (Fig. S3A) were increased with the FFC diet but were similar in the Veh-treated *vs.* LY-treated groups. Furthermore, LY treatment was well tolerated, and the physical activity, respiratory quotient, metabolic rate, and percentage of lean and fat masses when assessed by the comprehensive laboratory animal monitoring system and echo-magnetic resonance imaging were also similar between the Veh and LY treatment groups on the FFC diet (Fig. S3B and C). Furthermore, the liver-to-body weight ratio (Fig. 4B) and hepatic triglyceride content (Fig. 4C) in the FFC mice were reduced by LY treatment. However, steatosis was not significantly reduced by LY treatment in MASH mice (Fig. 4D). This observation was confirmed by automated quantification of steatosis percentage on the whole digitized H&E-stained slides (Fig. S4A and B), as well as by steatosis scoring (Fig. S4C) by estimating the steatotic area percentage in five fields per mouse and then taking the average (score 1 [6–33%], score 2 [33–66%], score 3 [>66%]). Similarly, hepatocyte ballooning was not altered by LY treatment (Fig. S4D). Taken together, these data suggest a minor role for GSK3 inhibition in steatosis and other metabolic alterations in murine MASH.

Given the key role of LSEC GSK3 in myeloid cell adhesion and TEM (Fig. 3E and F), we examined whether GSK3 inhibition reduces macrophage and neutrophil hepatic infiltration. Immunostaining of liver tissues indicated that LY-treated mice had a reduced positive area for the macrophage marker F4/80 (Fig. 4E) and the neutrophil marker myeloperoxidase (MPO) (Fig. S5A). Interestingly, the expression of the LSEC endotheliopathy marker ICAM-1 (Fig. 4F) was increased with FFC feeding and reduced with LY treatment, whereas the marker of differentiated LSEC Lyve-1 was reduced in FFC mice and restored with LY treatment (Fig. S5B). Similarly, *Cxcl2* mRNA expression increased with the FFC diet and decreased with LY treatment (Fig. 4G). These data support the role of GSK3 in the proinflammatory phenotypes of LSECs in MASH and are consistent with our *in vitro* findings.

Moreover, FFC-induced liver injury was attenuated by GSK3 inhibition as assessed by reduced plasma alanine aminotransferase (ALT) levels (Fig. 4H) and apoptotic hepatocytes by terminal deoxynucleotidyl transferase dUTP nick-end labeling (TUNEL)-positive cells (Fig. 4I) in LY-treated mice.

Finally, to determine whether GSK3 inhibition can mitigate liver fibrosis, the most important factor associated with morbidity and mortality in MASH,[32] we performed ultrasound-based liver elastography 4 weeks after the initiation of treatment with LY. Liver stiffness was assessed by the Young's modulus (YM), which was increased in FFC-fed mice but reduced with LY treatment (Fig. 5A). Likewise, FFC-fed LY-treated mice showed a reduced Sirius Red-positive area compared with Veh-treated mice on the same diet when quantified by morphometry (Fig. 5B), indicating a therapeutic effect of LY against MASH-associated liver fibrosis. Similarly, fiber density (when assessed by CT-FIRE, an academic software package available as a free download developed by the Eliceiri lab at UW Madison) was reduced in FFC-fed mice treated with LY (p <0.01; Fig. 5C). Overall, collagen fiber density was positively correlated with YM (Pearson's correlation coefficient, r = 0.70) (Fig. 5D). Collagen fibers were narrower and longer with the FFC diet than with the chow controls, with no change in straightness in the FFC treatment group *vs.* no treatment group (Fig. S6). These findings were further confirmed by immunostaining of the liver for alpha-smooth muscle actin (α-SMA), a hepatic stellate cell activation marker (Fig. 5E), and mRNA expression of the genes encoding α-SMA (*Acta2*) and Collagen 1a1 (*Col1a1*) (Fig. 5F). Taken together, these findings suggest that pharmacological inhibition of GSK3 ameliorates liver inflammation, injury, and fibrosis in diet-induced MASH.

GSK3 inhibition with elraglusib (9-ING-41) ameliorates CDHFD-induced murine MASH

To further confirm the role of GSK3β in the recruitment of proinflammatory myeloid cells to the liver, we used 9-ING-41, a more selective GSK3β inhibitor that is structurally distinct from LY [at 10 μM, 9-ING-41 was found to inhibit GSK3β by 97% and GSK3α by 92% (GSK3β IC_{50} = 635 nM)]. To validate our findings in a different MASH mouse model, we used a choline-deficient high-fat diet (CDHFD; A06071302, Research Diet), a well-established MASH mouse model that induces pronounced myeloid cell-associated liver inflammation and fibrosis in 6 weeks.[7,33] Mice were treated with either Veh or 9-ING-41 at a dose of 30 mg/kg per day intraperitoneally for 2 weeks during the final 2 weeks of the feeding study (Fig. 6A). The liver-to-body weight ratio was not altered by 9-ING-41 treatment in CDHFD-fed mice (Fig. S7A). Steatosis, lobular inflammation, and hepatocyte ballooning were assessed using the NASH Clinical Research Network Scoring System (NAS), which was reduced in CDHFD-fed 9-ING-41-treated mice (Fig. 6B and Fig. S7B), mainly secondary to reduced inflammation. Immunofluorescence and confocal microscopy showed increased neutrophil infiltration in CDHFD-fed mice when assessed by MPO staining, which was reduced with 9-ING-41 treatment (Fig. 6C). Likewise, immunostaining of liver tissues revealed that 9-ING-41-treated mice had a reduced positive area for macrophage marker F4/80 (Fig. 6D). Moreover, the mRNA expression of the proinflammatory monocyte marker Ccr2 increased with the CDHFD diet and decreased with 9-ING-41 treatment (Fig. 6E), suggesting that inhibition of GSK3 reduces myeloid cell infiltration in the MASH liver parenchyma. Furthermore, 9-ING-41 treatment reduced liver injury, as

assessed by ALT levels (Fig. 6F). Monocyte adhesion to LSECs increased in the LSECs of Veh-treated MASH mice and decreased in LSECs from 9-ING-41-treated MASH mice (Fig. 6G and Fig. S7C). However, pharmacological GSK3 inhibition did not significantly reduce the migration of bone marrow-derived monocytes isolated from mice with MASH (Fig. 6H) or subjected to the chemokine CCL2 (Fig. S8), suggesting a minor direct effect of GSK3 inhibition on monocyte recruitment.

To further examine the contribution of the different immune cells to the protective effect of GSK3 inhibition in MASH, we used mass cytometry by time of flight (CyTOF) using the Fluidigm Helios System, which allows comprehensive profiling of intrahepatic leukocyte (IHL) subpopulations based on multiple cell markers. Thirty-one clusters were obtained (Fig. 7A) on isolated IHLs from mice from the different experimental groups based on the intensities of 32 different cell surface markers and two

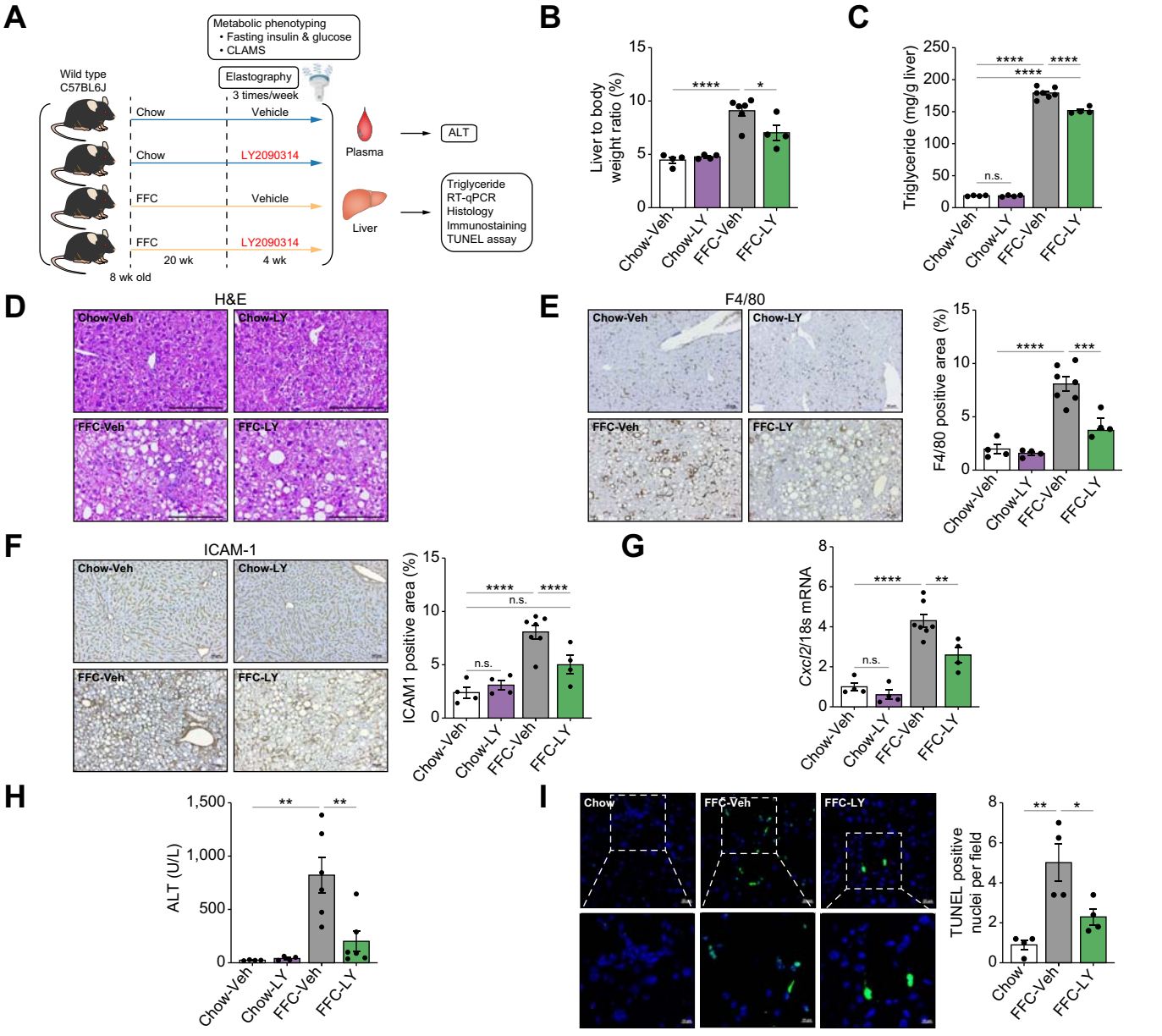

Fig. 4. Glycogen synthase kinase (GSK)-3 inhibition ameliorates liver injury and inflammation in fat, fructose, and cholesterol (FFC) diet-induced murine metabolic dysfunction-associated steatohepatitis (MASH). Wild-type (WT) C57BL/6J mice were fed either a chow or FFC diet for 24 weeks and treated with either vehicle (Veh) or the GSK3 inhibitor LY2090314 (LY) intraperitoneally 10 mg/kg three times per week for 4 weeks. (A) Schematic of the feeding experiment. (B) Liver-to-body weight ratio. (C) Liver triglyceride content. (D) Representative images of H&E staining of the liver sections. (E) Representative images of F4/80 immunostaining of the liver sections (left). F4/80-positive areas were quantified in five random 10 × microscopic fields and averaged for each animal (right). (F) Representative images of intracellular adhesion molecule 1 (ICAM-1) immunostaining in liver sections (left). ICAM-1-positive area is quantified (right). (G) Hepatic mRNA expression of C-X-C motif chemokine ligand 2 (*Cxcl2*). (H) Plasma alanine aminotransferase (ALT) level. (I) Representative images of terminal deoxynucleotidyl transferase dUTP nick-end labeling (TUNEL) staining of the liver sections (left). Quantification of TUNEL-positive cells (right). The marked boxes in the top images indicate the magnified images at the bottom. Bar graphs represent the mean ± SEM; $^{*}p$ <0.05, $^{**}p$ <0.01, $^{***}p$ <0.001, $^{****}p$ <0.0001, ns, non-significant (one-way ANOVA with Bonferroni's multiple comparison; n = 4–7). Scale bars: 10 μm (I, insets), 20 μm (I), 50 μm (E,F), 100 μm (D).

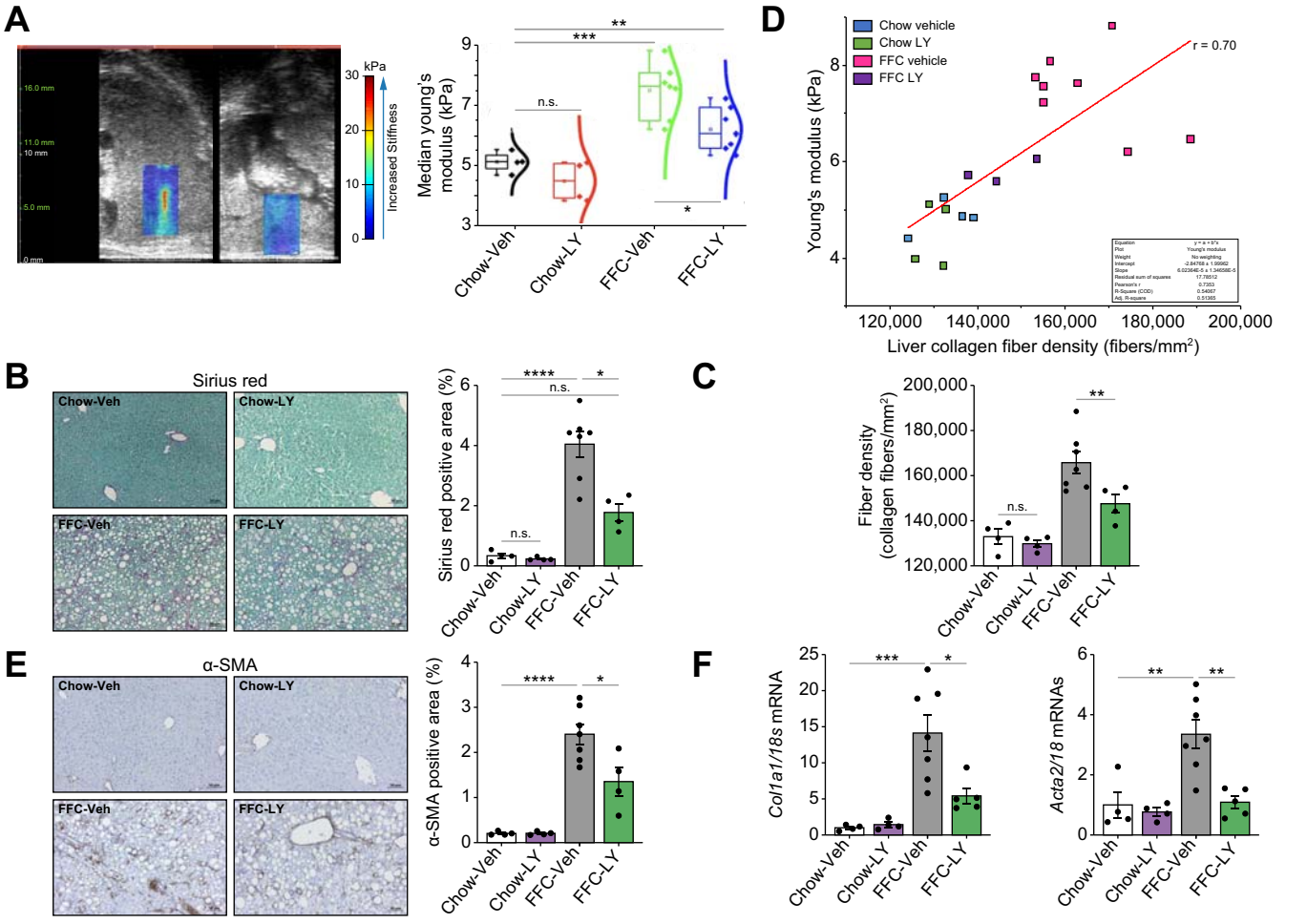

Fig. 5. Glycogen synthase kinase (GSK)-3 inhibition by LY2090314 (LY)-ameliorated liver fibrosis in diet-induced murine metabolic dysfunction-associated steatohepatitis (MASH). (A) Ultrasound images of the liver using shear wave elastography segmentation overlay. Median Young's modulus (kPa) of the vehicle (Veh) and LY-treated mice fed chow or a fat, fructose, and cholesterol (FFC) diet. (B) Representative images of Sirius Red staining of liver sections (left). Sirius Red-positive areas were quantified in five random 10 × microscopic fields and averaged for each animal (right). (C) *Ex vivo* validation of collagen fiber density after the final time point using CT-FIRE (left). (D) Correlation between *in vivo* ultrasound and *ex vivo* CT-FIRE measurements of liver fibrosis pooled across all groups. Pearson's r correlation = 0.7 (right). (E) Representative images of alpha-smooth muscle actin (α-SMA) immunostaining (left) and quantification (right) of liver sections. (F) α-SMA and Collagen1α1 mRNA expression levels. Bar graphs represent mean ± SEM; **p* <0.05, ***p* <0.01, ****p* <0.001, *****p* <0.0001, ns, non-significant (one-way ANOVA with Bonferroni's multiple comparison; n = 4–7). Scale bars: 50 μm (B,E).

cytosolic markers (S100A8 and MPO) (Fig. 7A and B; Tables S1 and S2, and Fig. S9), which allowed comprehensive profiling of the phenotype, differentiation, and function of the intrahepatic subpopulations of innate and adaptive immune cells. t-Distributed stochastic neighbor embedding (tSNE) plots of each experimental group were analyzed, with red indicating high-frequency categorization of cells to a cluster and blue indicating low frequency (Fig. 7C). Our data indicate that the cell percentages of clusters 31 and 6, representing monocyte-derived dendritic cells (MoDCs) (Fig. 7D and E), and cluster 9, comprising proinflammatory monocyte-derived macrophages (MoMFs) (Fig. 7F), increased with the CDHFD diet and decreased with 9-ING-41 treatment. However, 9-ING-41 treatment in CDHFD-fed mice did not significantly alter the percentage of other intrahepatic immune cell subpopulations in the remaining clusters (Fig. S10), further confirming that GSK3 inhibition reduces circulating myeloid cell infiltration and proinflammatory differentiation in the MASH liver.

To further study the effects of GSK3 inhibitor on liver fibrosis in MASH, we performed Sirius Red staining, which showed a reduction in Sirius Red-positive area in the CDHFD-fed 9-ING-41-treated mice compared with Veh-treated mice on the same diet (Fig. 8A). Likewise, these findings were replicated with immunostaining for α-SMA (Fig. 8B), and measurement of *Col1a1* mRNA expression (Fig. 8C), indicating a protective effect of 9-ING-41 against MASH-associated liver fibrosis. Taken together, these findings suggest that pharmacological inhibition of GSK3 by 9-ING-41 in CDHFD-induced murine MASH ameliorates liver inflammation, injury, and fibrosis.

Discussion

The current study provides insight into the role of GSK3 in lipotoxicity-induced LSEC endotheliopathy in MASH. Herein, we demonstrate that: (i) in LSECs isolated from mice with diet-induced MASH, leukocyte TEM and focal adhesion are among

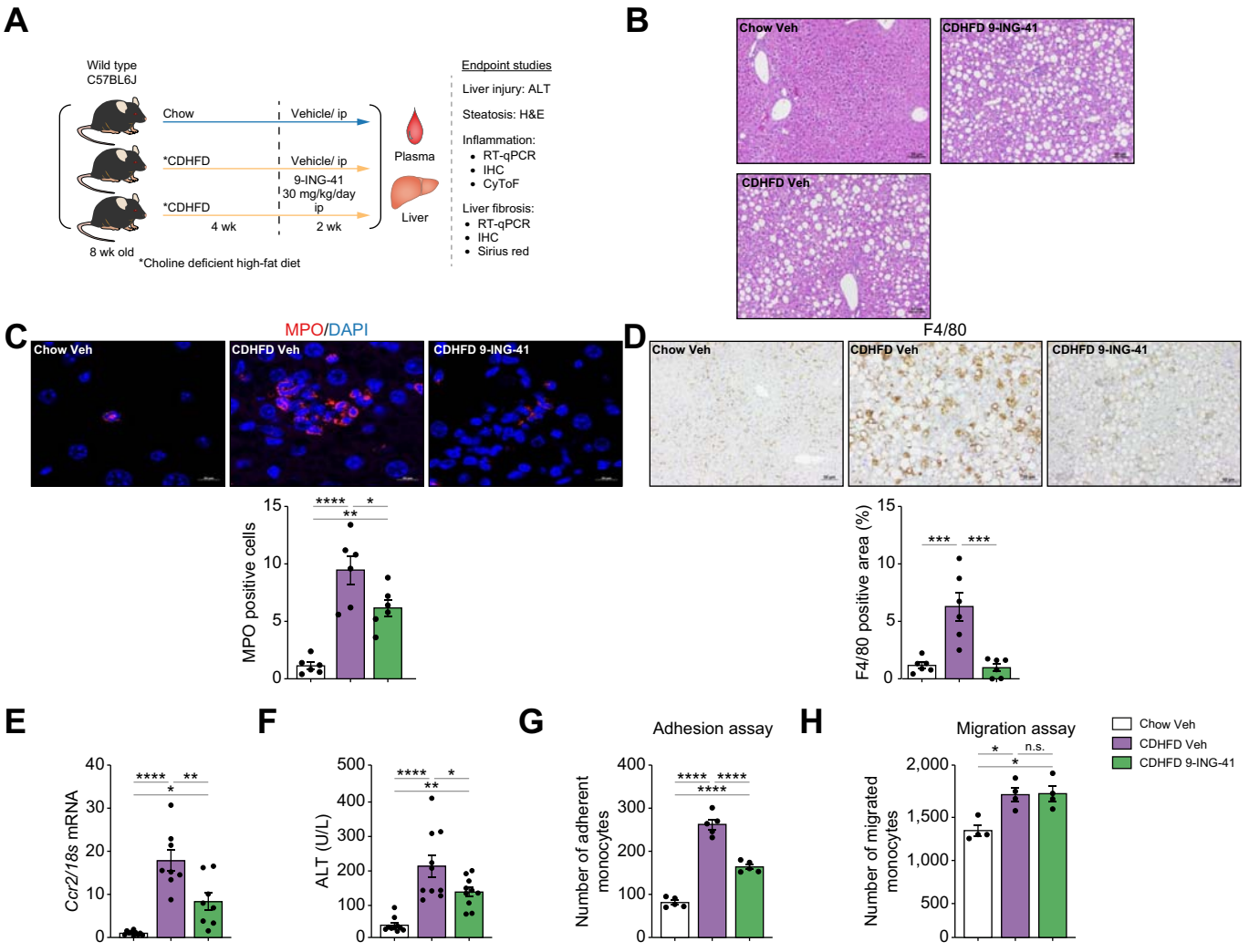

Fig. 6. Glycogen synthase kinase (GSK)-3 inhibition with elraglusib improves liver injury and inflammation in choline-deficient high-fat diet (CDHFD)-induced murine metabolic dysfunction-associated steatohepatitis (MASH). Eight-week-old wild-type (WT) C57BL/6J mice were fed either a chow diet or CDHFD for 6 weeks and treated with either vehicle (Veh) or the GSK3 inhibitor 9-ING-41 (intraperitoneally 30 mg/kg daily for 2 weeks). (A) Schematic of the feeding experiment. (B) Representative images of H&E staining of the liver sections. (C) Myeloperoxidase (MPO) immunofluorescence staining (red) Nuclei were stained with DAPI (blue). Images are shown at a 63 × magnification. (D) F4/80 immunostaining of liver sections (left). F4/80-positive areas were quantified in five random 10 × microscopic fields and averaged for each animal (right). (E) Hepatic mRNA expression levels of *Ccr2*. (F) Plasma alanine aminotransferase (ALT) levels (n = 5–10). Quantification of (G) monocytes adherent to liver sinusoidal endothelial cells (LSECs) (n = 5), (H) and migrating monocytes (n = 3) in the different experimental groups. Bar graphs represent mean ± SEM; *p <0.05, **p <0.01, ***p <0.001, ****p <0.0001, ns, non-significant (one-way ANOVA with Bonferroni's multiple comparison). Scale bars: 10 μm (C), 50 μm (B,D).

the major altered pathways in differentially expressed proteomics and transcriptomics; (ii) based on kinome profiling, GSK3 is the central hub kinase associated with MASH pathogenesis in LSECs; (iii) GSK3 drives the toxic lipid-induced proinflammatory phenotype in LSECs; and (iv) pharmacological inhibition of GSK3, using two distinct pharmacological inhibitors and two different mouse models of MASH, ameliorates liver inflammation, injury, and fibrosis mainly by reducing myeloid cell infiltration and proinflammatory differentiation in the MASH liver.

Given that protein phosphorylation is central to dynamic biological processes, including metabolic and immune responses, multiple liver phosphoproteomic studies have shed light on the key mediators of metabolic liver diseases. For example, pathway analysis of the liver phosphoproteome of patients with MASH and simple steatosis identified carbohydrate metabolism as a significant biological process relevant to MASH progression.[34] In another liver phosphoproteomics study using a murine model of alcohol-associated liver disease, the apoptosis signal-regulating kinase 1 (ASK1)–p38 axis was identified as a downstream target of the pro-necroptotic protein receptor-interaction protein kinase 3 (RIP3).[35] These whole-liver phosphoproteomic studies likely reflect signaling alterations in hepatocytes. To the best of our knowledge, the current study is the first to examine the phosphoproteome of LSECs, the most abundant and highly immunogenic cell population among non-parenchymal liver cells. Notably, none of the previous liver phosphoproteomic studies detected GSK3 as a signaling hub, which implies that an LSEC-specific kinase-driven signaling network exists in the context of metabolic perturbations in the liver. Moreover, a previous study reported that the phosphorylation levels of GSK3 in adipose tissue are one of the predictors of advanced liver fibrosis in patients with metabolic dysfunction-associated

steatotic liver disease (MASLD).[36] Taken together, these studies suggest that altered GSK3 activation is a common driver in the pathophysiology of metabolic syndrome (MS) across multiple organs.

Our study identified *ICAM1* and *CXCL2* as downstream targets of GSK3 in LSECs; interestingly, both ICAM-1 and CXCL2 are prerequisites for circulating leukocyte TEM and recruitment to inflamed tissue.[37,38] Moreover, pathway analysis of the multi-omics data sets on LSECs from murine MASH identified focal adhesion and leukocyte TEM as significant biological processes in MASH progression, further implicating *ICAM1* and *CXCL2* in MASH pathogenesis. Likewise, we identified a GSK3-dependent increase in VE-cadherin phosphorylation in LSECs under lipotoxic stress, promoting immune cell TEM. However, VE-cadherin phosphorylation and internalization can also modulate endothelial growth factor receptor function, cell survival

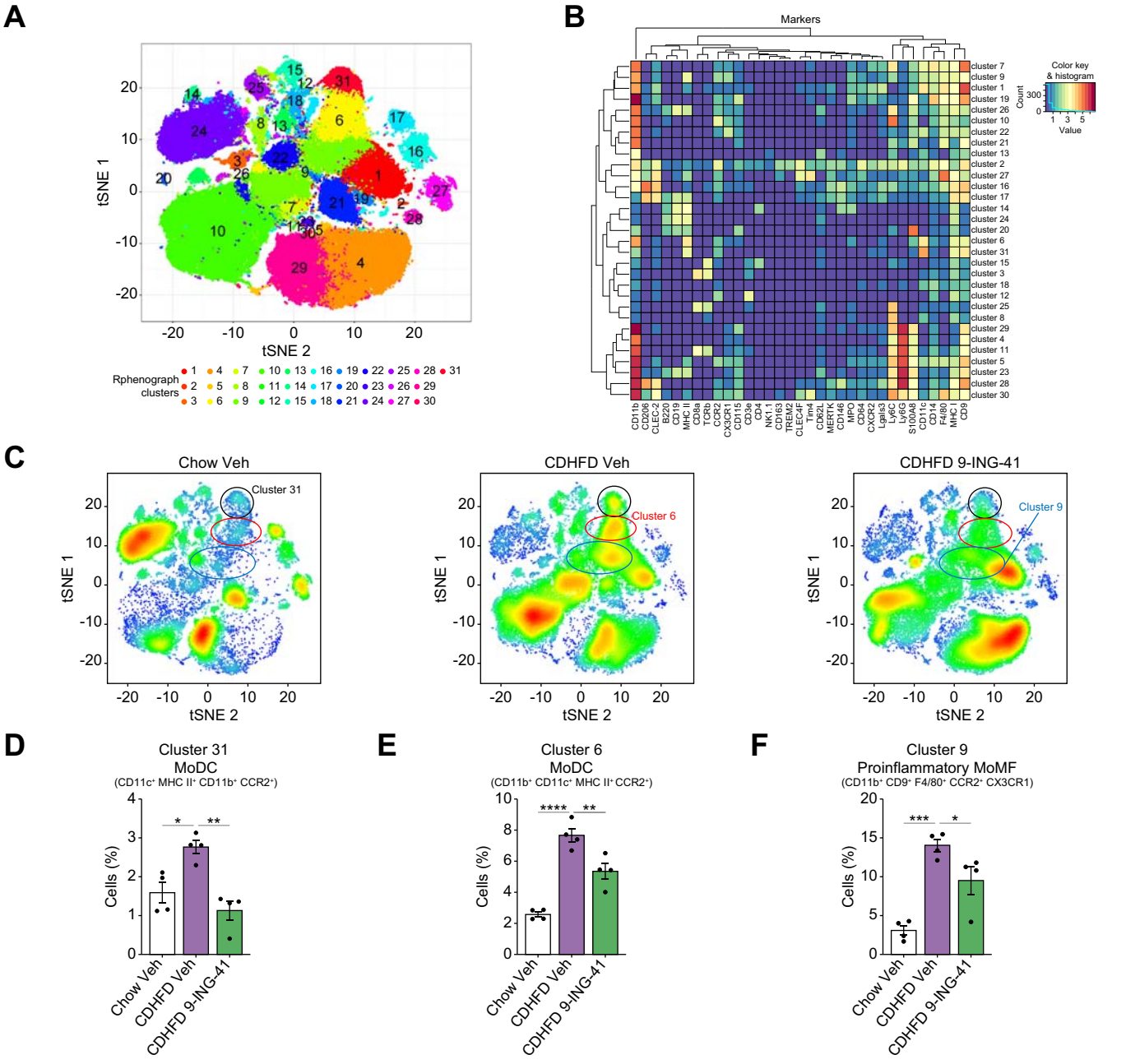

Fig. 7. Glycogen synthase kinase (GSK)-3 inhibition with elraglusib attenuates the recruitment of proinflammatory myeloid cells in the liver of choline-deficient high-fat diet (CDHFD)-fed mice. Cytometry by time of flight (CyTOF) was performed on intrahepatic leukocytes (IHLs) of chow-fed mice and CDHFD-fed mice treated with the GSK3 inhibitor elraglusib (9-ING-41). (A) Thirty-one unique clusters were defined by a panel of 32 cell-surface markers, including CD45 and two intracellular markers (myeloperoxidase [MPO] and S100A8) using the Rphenograph clustering algorithm and visualized on a tSNE plot. (B) Heatmap demonstrating the distribution and relative intensity of the markers used in clustering analysis. (C) Representative tSNE plots of each experimental group. Red indicates high-frequency categorization of cells into a cluster, and blue indicates low frequency. Clusters 31 (D) and 6 (E) are consistent with monocyte-derived dendritic cells (MoDCs), whereas cluster 9 (F) is consistent with proinflammatory monocyte-derived macrophages (MoMFs). Bar graphs represent the mean ± SEM; *p <0.05, **p <0.01, ***p <0.001, ****p <0.0001 (one-way ANOVA with Bonferroni's multiple comparison; n = 4). tSNE, t-distributed stochastic neighbor embedding.

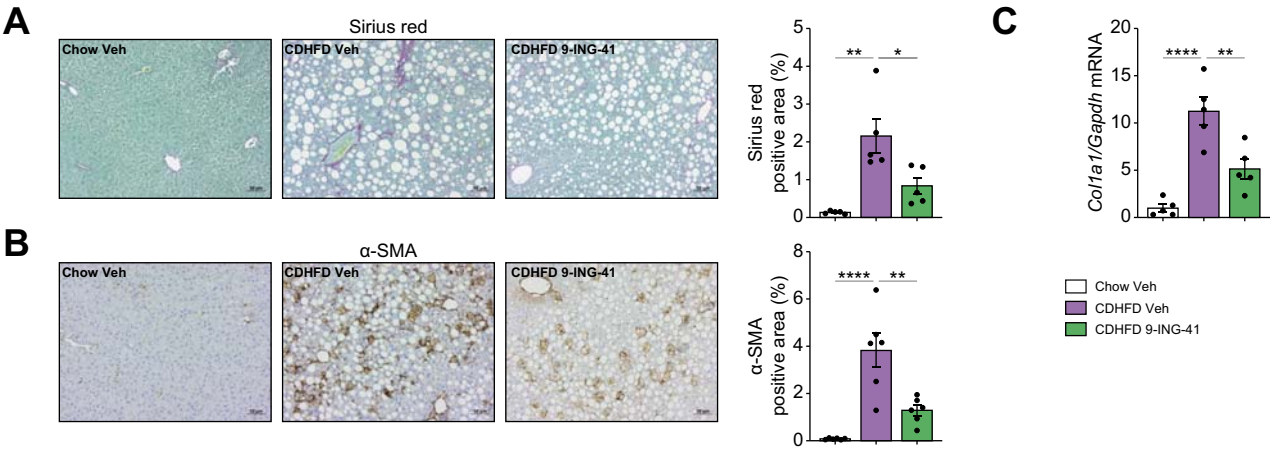

Fig. 8. Elraglusib (9-ING-41) treatment in choline-deficient high-fat diet (CDHFD)-fed mice attenuates liver fibrosis. (A) Representative images of Sirius Red staining of liver sections (left). Sirius Red-positive areas were quantified (right). (B) Representative images of α-SMA immunostaining of the liver sections (left). α-SMA-positive areas were quantified (right). (C) Hepatic mRNA expression levels of collagen 1α1 were assessed. Bar graphs represent the mean ± SEM; **p* <0.05, ***p* <0.01, *****p* <0.0001 (one-way ANOVA with Bonferroni's multiple comparison) (n = 5 or 6). Scale bars: 50 μm (A,B).

through the PI3K/AKT signaling pathway, cell proliferation via the ERK/MAPK pathway, and cell migration via the GTPase RhoA pathway.[39] Hence, these pathways are potentially implicated in lipotoxic endotheliopathy.

ICAM-1 is an adhesion molecule of the Ig superfamily and is predominantly expressed in endothelial cells. It has been shown previously that toxic lipids induce aberrant expression of the other Ig superfamily member, vascular cell adhesion molecule 1 (VCAM1), in LSECs, and that endothelial cell-specific genetic deletion or pharmacological inhibition of VCAM1 ameliorates murine MASH.[7] In addition, CXCL2, along with other CXCL chemokines, has been implicated in leukocyte chemotaxis via its cognate binding interaction with CXC motif chemokine receptor 2 (CXCR2), a typical G-protein-coupled receptor.[40] Increased levels of CXCL2 have been observed in the serum of individuals with obesity.[41] CXCL2 shares 90% amino acid sequence similarity with the related chemokine CXCL1, the biological function of which has been studied extensively.[40,42] It is intriguing that, in our NanoString-based gene expression analysis, *CXCL2*, but not *CXCL1*, was among the 'lipotoxic stress-dependent' and 'GSK3-dependent' genes, suggesting the different transcriptional regulation mechanisms between these two molecules. Furthermore, the expression of *CXCL2* was reduced by the GSK3 inhibitor LY in murine MASH, suggesting that LSEC GSK3 signaling in MASH is also implicated in chemotaxis.

Although the two isoforms of GSK3 (α and β) share 85% amino acid sequence homology,[43] whole-body GSK3β-knockout mice are embryonically lethal, whereas GSK3α-knockout mice are viable, indicating that these two isoforms have non-redundant functions.[44,45] Recently, pharmacological inhibition of GSK3 or endothelial cell-specific deletion of GSK3β was reported to reduce atherosclerotic calcification in *Apoe*$^{-/-}$ Western diet-fed mice.[46] In another murine atherosclerosis model, deletion of endothelial GSK3α, but not GSK3β, attenuated atherosclerosis, which was associated with reduced endothelial adhesion molecule expression and monocyte recruitment to the vascular wall.[47] Despite several similarities, one of the differences between this and the current study is that GSK3α-deleted endothelial cells had decreased expression of VCAM1 *in vivo*, whereas, in the current study, GSK3 inhibition reduced the expression of ICAM-1 *in vitro* and *in vivo*. This discrepancy might be secondary to the differences between vascular endothelial cells and LSECs, which are specialized fenestrated endothelial cells. Furthermore, GSK3 inhibitors suppress the kinase activity of both GSK3α and GSK3β because of the extremely high amino acid homology in the kinase domain of these two isoforms.[48] Taken together, these studies suggest that GSK3 inhibition would have a beneficial effect on extrahepatic vascular manifestations of MS, further supporting the involvement of GSK3 in endothelial inflammation. Ongoing experiments are exploring the distinct role of GSK3β *vs.* GSK3α in LSECs *vs.* hepatocytes in murine MASH, and their role in disease development and progression, which are beyond the scope of the current manuscript.

Nevertheless, our *in vivo* studies demonstrated that GSK3 inhibitors are well tolerated and elicit robust improvements in liver inflammation, injury, and fibrosis in diet-induced murine MASH, which, from a clinical perspective, might be as informative as findings obtained from genetically engineered mouse models. In addition, GSK3 inhibitors have been safely and effectively used for decades in mood disorders[49] and, therefore, could be repurposed for MASH therapy.

Collectively, our study implicates GSK3 in the proinflammatory phenotype of LSECs in MASH and provides preclinical data to support targeting GSK3 as a novel anti-inflammatory and antifibrotic therapeutic approach in human MASH.

Abbreviations

α-SMA, alpha-smooth muscle actin; ALT, alanine aminotransferase; ASK1, apoptosis signal-regulating kinase 1; CDHFD, choline-deficient high fat diet; CXCL2, C-X-C motif chemokine ligand 2; CXCR2, CXC motif chemokine receptor 2; CyTOF, cytometry by time of flight; FAK, focal adhesion kinase; FFA, free fatty acid; FFC, fat, fructose and cholesterol; GAPDH, glyceraldehyde-3-phosphate dehydrogenase; GS, glycogen synthase; GSK3, glycogen synthase kinase 3; HOMA-IR, Homeostatic Model

Assessment for Insulin Resistance; ICAM-1, intracellular adhesion molecule 1; IHL, intrahepatic leukocyte; KEGG, Kyoto Encyclopedia of Genes and Genomes; LPC, lysophosphatidylcholine; LSEC, liver sinusoidal endothelial cell; LY, LY2090314; MASH, metabolic dysfunction associated steatohepatitis; MASLD, metabolic dysfunction-associated steatotic liver disease; MoDC, monocyte-derived dendritic cells; MoMF, monocyte-derived macrophage; MPO, myeloperoxidase; MS, metabolic syndrome; NAS, NASH Clinical Research Network Scoring System; p-GS, phosphorylated glycogen synthase; PA, palmitate; qPCR, quantitative PCR; RIP3, receptor-interacting protein kinase 3; RNA-seq, RNA-sequencing; siRNA, small interfering RNA; TEM, transendothelial migration; TNF-α, tumor necrosis factor-α; TSEC, transformed mouse liver sinusoidal endothelial cell; tSNE, t-distributed stochastic neighbor embedding; TUNEL, terminal deoxynucleotidyl transferase dUTP nick-end labeling; VCAM1, vascular cell adhesion molecule 1; VE-cadherin, vascular endothelial cadherin; Veh, vehicle; WT, wild-type; YM, Young's modulus.

Financial support
The research reported in this publication was supported by the Mayo Foundation and the National Institute of Diabetes and Digestive and Kidney Diseases (NIDDK) of the National Institutes of Health (NIH) under Award R01DK122948 to SHI, NIH shared instruments grant (S10OD028633), and P30DK084567 to the Mayo Clinic Center for Cell Signaling in Gastroenterology, and JSPS Overseas Research Fellowships to KF Support was also provided to PH by NIDDK NIH under Award R01DK130884; to HL by the Mayo Clinic Cancer Center (P30CA015083), David F. and Margaret T. Grohne Cancer Immunology and Immunotherapy Program, Mayo Center for Biomedical Discovery, Center for Individualized Medicine, and Eric & Wendy Schmidt Fund for AI Research & Innovation; to AOB by NIDDK NIH under Award K01DK124358; to CRS from the Zell Family Foundation; to MFR from R43DK126607; and to CM by an Innovation grant ADL0048, sponsored by the Department of Laboratory Medicine and Pathology Translational Research, Innovation and Test Development Office (TRITDO) and the Center for Individualized Medicine (CIM) at the Mayo Clinic.

Conflicts of interest
The authors declare no conflicts of interest.

Please refer to the accompanying ICMJE disclosure forms for further details.

Authors' contributions
Concept formulation: SHI. Designed research studies: MK, QG, KF, SHI. Conducted experiments: MK, QG, KF, HSKL, KW, LVP, SI. Acquired data: MK, QG, KF, HSKL, HH, SI. Analyzed data: MK, QG, KF, CC, HSKL, HH, MR, CS, KP, HL, SI, SHI. Designed and implemented the AI algorithm for liver zonation and steatosis quantification: CM. Designed software for automatic quantification of steatosis on digitized slides: IK, Y–KN. Provided materials: AM, AOB, PH. Drafted manuscript: MK, QG, KF, CC, SHI. Revised manuscript: CC, AM, AOB, PH, HH, MR, CS, KP, HL, SHI.

Data availability statement
RNA-seq data on isolated mouse LSECs were deposited in the Gene Expression Omnibus database (GSE164006); proteomics and phosphoproteomics data on isolated mouse LSECs were deposited in the ProteomeXchange Consortium via the PRIDE partner repository (PXD048073).

Acknowledgements
The authors thank Gregory J. Gores for his scientific insight and acknowledge the assistance of the Proteomic Core at Mayo Clinic led by Akhilesh Pandey.

Supplementary data
Supplementary data to this article can be found online at https://doi.org/10.1016/j.jhepr.2024.101073.

References
Author names in bold designate shared co-first authorship

[1] Younossi ZM. Non-alcoholic fatty liver disease – a global public health perspective. J Hepatol 2019;70:531–544.
[2] Neuschwander-Tetri BA. Hepatic lipotoxicity and the pathogenesis of nonalcoholic steatohepatitis: the central role of nontriglyceride fatty acid metabolites. Hepatology 2010;52:774–788.
[3] Friedman SL, Neuschwander-Tetri BA, Rinella M, et al. Mechanisms of NAFLD development and therapeutic strategies. Nat Med 2018;24:908–922.
[4] McConnell MJ, Kostallari E, Ibrahim SH, et al. The evolving role of liver sinusoidal endothelial cells in liver health and disease. Hepatology 2023;78:649–669.
[5] Ibrahim SH. Sinusoidal endotheliopathy in nonalcoholic steatohepatitis: therapeutic implications. Am J Physiol Gastrointest Liver Physiol 2021;321:G67–G74.
[6] Furuta K, Tang X, Islam S, et al. Endotheliopathy in the metabolic syndrome: mechanisms and clinical implications. Pharmacol Ther 2023;244:108372.
[7] Furuta K, Guo Q, Pavelko KD, et al. Lipid-induced endothelial vascular cell adhesion molecule 1 promotes nonalcoholic steatohepatitis pathogenesis. J Clin Invest 2021;131:e143690.
[8] Miyachi Y, Tsuchiya K, Komiya C, et al. Roles for cell-cell adhesion and contact in obesity-induced hepatic myeloid cell accumulation and glucose intolerance. Cell Rep 2017;18:2766–2779.
[9] **Guo Q**, **Furuta K**, Islam S, et al. Liver sinusoidal endothelial cell expressed vascular cell adhesion molecule 1 promotes liver fibrosis. Front Immunol 2022;13:983255.
[10] Ritz T, Krenkel O, Tacke F. Dynamic plasticity of macrophage functions in diseased liver. Cell Immunol 2018;330:175–182.
[11] **Krenkel O**, **Hundertmark J**, Abdallah AT, et al. Myeloid cells in liver and bone marrow acquire a functionally distinct inflammatory phenotype during obesity-related steatohepatitis. Gut 2020;69:551–563.
[12] **McNamara HA**, **Cockburn IA**. The three rs: recruitment, retention and residence of leukocytes in the liver. Clin Trans Immunol 2016;5:e123.
[13] Miyao M, Kotani H, Ishida T, et al. Pivotal role of liver sinusoidal endothelial cells in NAFLD/NASH progression. Lab Invest 2015;95:1130–1144.
[14] **Guo Q**, **Furuta K**, Lucien F, et al. Integrin beta1-enriched extracellular vesicles mediate monocyte adhesion and promote liver inflammation in murine NASH. J Hepatol 2019;71:1193–1205.
[15] Muller WA. Transendothelial migration: unifying principles from the endothelial perspective. Immunol Rev 2016;273:61–75.
[16] Shetty S, Lalor PF, Adams DH. Liver sinusoidal endothelial cells – gatekeepers of hepatic immunity. Nat Rev Gastroenterol Hepatol 2018;15:555–567.
[17] Beurel E, Grieco SF, Jope RS. Glycogen synthase kinase-3 (GSK3): regulation, actions, and diseases. Pharmacol Ther 2015;148:114–131.
[18] Jeffers A, Qin W, Owens S, et al. Glycogen synthase kinase-3beta inhibition with 9-ING-41 attenuates the progression of pulmonary fibrosis. Sci Rep 2019;9:18925.
[19] **Ramirez SH**, **Fan S**, Zhang M, et al. Inhibition of glycogen synthase kinase 3beta (GSK3beta) decreases inflammatory responses in brain endothelial cells. Am J Pathol 2010;176:881–892.
[20] **Yi L**, **Huang X**, Guo F, et al. GSK-3beta-dependent activation of GEF-H1/ROCK signaling promotes LPS-induced lung vascular endothelial barrier dysfunction and acute lung injury. Front Cel Infect Microbiol 2017;7:357.
[21] Nakamura M, Liu T, Husain S, et al. Glycogen synthase kinase-3alpha promotes fatty acid uptake and lipotoxic cardiomyopathy. Cell Metab 2019;29:1119–1134.
[22] Gutierrez Sanchez LH, Tomita K, Guo Q, et al. Perinatal nutritional reprogramming of the epigenome promotes subsequent development of nonalcoholic steatohepatitis. Hepatol Commun 2018;2:1493–1512.
[23] Furuta K, Guo Q, Hirsova P, et al. Emerging roles of liver sinusoidal endothelial cells in nonalcoholic steatohepatitis. Biology 2020;9:395.
[24] **Lachmann A**, **Ma'ayan A**. KEA: kinase enrichment analysis. Bioinformatics 2009;25:684–686.
[25] de Almeida IT, Cortez-Pinto H, Fidalgo G, et al. Plasma total and free fatty acids composition in human non-alcoholic steatohepatitis. Clin Nutr 2002;21:219–223.
[26] Hughes K, Nikolakaki E, Plyte SE, et al. Modulation of the glycogen synthase kinase-3 family by tyrosine phosphorylation. EMBO J 1993;12:803–808.
[27] Kakisaka K, Cazanave SC, Fingas CD, et al. Mechanisms of lysophosphatidylcholine-induced hepatocyte lipoapoptosis. Am J Physiol Gastrointest Liver Physiol 2012;302:G77–G84.
[28] Kolhe R, Ghilzai U, Mondal AK, et al. Nanostring-based identification of the gene expression profile in trigger finger samples. Healthcare (Basel) 2021;9:1592.

[29] Wang W, Lollis EM, Bordeleau F, et al. Matrix stiffness regulates vascular integrity through focal adhesion kinase activity. FASEB J 2019;33:1199–1208.
[30] Sullivan DP, Dalal PJ, Jaulin F, et al. Endothelial IQGAP1 regulates leukocyte transmigration by directing the LBRC to the site of diapedesis. J Exp Med 2019;216:2582–2601.
[31] Gray JE, Infante JR, Brail LH, et al. A first-in-human phase I dose-escalation, pharmacokinetic, and pharmacodynamic evaluation of intravenous LY2090314, a glycogen synthase kinase 3 inhibitor, administered in combination with pemetrexed and carboplatin. Invest New Drugs 2015;33:1187–1196.
[32] Ekstedt M, Hagström H, Nasr P, et al. Fibrosis stage is the strongest predictor for disease-specific mortality in NAFLD after up to 33 years of follow-up. Hepatology 2015;61:1547–1554.
[33] Matsumoto M, Hada N, Sakamaki Y, et al. An improved mouse model that rapidly develops fibrosis in non-alcoholic steatohepatitis. Int J Exp Pathol 2013;94:93–103.
[34] Wattacheril J, Rose KL, Hill S, et al. Non-alcoholic fatty liver disease phosphoproteomics: a functional piece of the precision puzzle. Hepatol Res 2017;47:1469–1483.
[35] Singh V, Huang E, Pathak V, et al. Phosphoproteomics identifies pathways underlying the role of receptor-interaction protein kinase 3 in alcohol-associated liver disease and uncovers apoptosis signal-regulating kinase 1 as a target. Hepatol Commun 2022;6:2022–2041.
[36] Younossi ZM, Baranova A, Stepanova M, et al. Phosphoproteomic biomarkers predicting histologic nonalcoholic steatohepatitis and fibrosis. J Proteome Res 2010;9:3218–3224.
[37] Girbl T, Lenn T, Perez L, et al. Distinct compartmentalization of the chemokines CXCL1 and CXCL2 and the atypical receptor ACKR1 determine discrete stages of neutrophil diapedesis. Immunity 2018;49:1062–1076.
[38] Arts JJG, Mahlandt EK, Gronloh MLB, et al. Endothelial junctional membrane protrusions serve as hotspots for neutrophil transmigration. Elife 2021;10:e66074.
[39] Nan W, He Y, Wang S, et al. Molecular mechanism of VE-cadherin in regulating endothelial cell behaviour during angiogenesis. Front Physiol 2023;14:1234104.
[40] Cheng Y, Ma XL, Wei YQ, et al. Potential roles and targeted therapy of the CXCLs/CXCR2 axis in cancer and inflammatory diseases. Biochim Biophys Acta Rev Cancer 2019;1871:289–312.
[41] Rouault C, Pellegrinelli V, Schilch R, et al. Roles of chemokine ligand-2 (CXCL2) and neutrophils in influencing endothelial cell function and inflammation of human adipose tissue. Endocrinology 2013;154:1069–1079.
[42] Vries MH, Wagenaar A, Verbruggen SE, et al. CXCL1 promotes arteriogenesis through enhanced monocyte recruitment into the peri-collateral space. Angiogenesis 2015;18:163–171.
[43] Woodgett JR. Molecular cloning and expression of glycogen synthase kinase-3/factor A. EMBO J 1990;9:2431–2438.
[44] Hoeflich KP, Luo J, Rubie EA, et al. Requirement for glycogen synthase kinase-3beta in cell survival and NF-kappaB activation. Nature 2000;406:86–90.
[45] MacAulay K, Doble BW, Patel S, et al. Glycogen synthase kinase 3alpha-specific regulation of murine hepatic glycogen metabolism. Cel Metab 2007;6:329–337.
[46] **Cai X**, **Zhao Y**, Yang Y, et al. GSK3beta inhibition ameliorates atherosclerotic calcification. Int J Mol Sci 2023;24:11638.
[47] **Mastrogiacomo L**, **Werstuck GH**. Investigating the role of endothelial glycogen synthase kinase3alpha/beta in atherogenesis in low density lipoprotein receptor knockout mice. Int J Mol Sci 2022;23:14780.
[48] Kaidanovich-Beilin O, Woodgett JR. GSK-3: functional insights from cell biology and animal models. Front Mol Neurosci 2011;4:40.
[49] Jope RS. Glycogen synthase kinase-3 in the etiology and treatment of mood disorders. Front Mol Neurosci 2011;4:16.